

# Sensitivity Study for Dark Matter Experiments Searching for Annual Modulation

Raymond T. Co  
Office of Science, Science Undergraduate Laboratory Internship Program

University of California, Berkeley

Fermi National Accelerator Laboratory  
Batavia, Illinois

August 13<sup>th</sup>, 2010

Prepared in fulfillment of the requirement of the Office of Science, Department of Energy's Science Undergraduate Laboratory Internship under the supervision of Drs. Jonghee Yoo and Lauren Hsu in the Particle Physics Division at Fermi National Accelerator Laboratory.

Participant: \_\_\_\_\_  
Signature

Research Advisors: \_\_\_\_\_  
Signature

\_\_\_\_\_  
Signature

## ABSTRACT

Sensitivity Study for Dark Matter Experiments Searching for Annual Modulation  
Raymond T. Co (University of California-Berkeley, Berkeley, CA 94720), Jonghee Yoo and  
Lauren Hsu (Fermi National Accelerator Laboratory, Batavia, IL 60510).

Dark matter (DM) is postulated to account for the “unseen” mass whose gravitational effects on galactic objects have been observed. Weakly interacting massive particles (WIMPs) are hypothetical particles serving as one of the solutions to the dark matter problem. We adopt the dark matter standard halo model (SHM) [1] in our galaxy in which the dark matter halo is nearly at rest relative to luminous matter in the Milky Way. Therefore, the flux of WIMPs depends on Earth’s motion relative to dark matter. DM experiments search for the recoil events of WIMPs on target materials. The SHM predicts that as Earth orbits the Sun, DM’s modulating relative velocity induces seasonal fluctuation in dark matter event rates. The dark matter experiment DAMA/LIBRA has sought for and claimed to observe such annual modulation signature. Nonetheless, the DAMA/LIBRA results are controversial because they are inconsistent with the null observations from other direct search experiments, such as CDMS and XENON100. As the modulation signal may be due to unknown background in the DAMA/LIBRA, different experiments are being proposed to cross-check the DAMA/LIBRA modulation. In its early stage, an experiment is being proposed in the Southern Hemisphere because seasonal fluctuations therein are 180 degrees out of phase with the Northern Hemisphere where the DAMA/LIBRA is located. In this paper, we first review and study the SHM in detail. We then further investigate several conditions for experiments to probe the DAMA/LIBRA allowed region. Assuming null observation of WIMP recoils and a Poisson distribution for background events, we study the effects of different exposure times, background levels, and energy thresholds on the limit curve. In order to rule out the DAMA/LIBRA allowed region at 90% confidence level, we find corresponding background and exposure conditions necessary for the proposed experiments that search for annual modulation.

## INTRODUCTION

The existence of dark matter has been proposed to account for 1. the discrepancies between the measured and calculated rotational velocities of stars [2], 2. the amount of mass needed to gravitationally bind clusters of galaxies [3], 3. the strong gravitational potential that traps the hot gas in clusters [4], and 4. the excess amount of galaxy masses that cause the gravitational lensing observed by sky surveys [5]. According to the concordance model, the measurements on the cosmic microwave [6], distance measurement from type Ia supernovae luminosity [7], and the large scale structure of the Universe [8–10], draw a conclusion that the Universe is comprised of 73% “dark energy”, 23% dark matter, and only 4% ordinary matter. Weakly interacting massive particles are hypothetical particles that serve as one of the solutions to account for the above dark matter phenomena. As implied by its name, the WIMP interacts with ordinary matter only through the weak force. WIMPs are predicted by many extensions to the standard model of particle physics. The lightest neutralino predicted by supersymmetric theories, naturally emerges to serve as a WIMP candidate [11].

In the SHM, the galaxy–trapped dark matter distribution is at rest relative to the luminous matter in the Milky Way. We also assume that the velocity spectrum of the dark matter follows a Maxwell–Boltzmann distribution, which is truncated at the Milky Way escape velocity. Dark matter experimental techniques fall into two categories– the indirect and direct searches. The indirect searches are generally subject to astrophysical uncertainties, but they can probe regions in parameter space that are inaccessible to the direct searches. In the indirect search, experiments search for the particles emitted from the annihilation of dark matter particle pairs. To directly search for dark matter, experiments aim to look for the nuclear recoils from a WIMP–nucleon interaction. In this paper, we focus our discussions on the direct search of dark matter.

As one of the direct search experiments, the Cryogenic Dark Matter Search (CDMS) experiment searches for WIMPs with germanium and silicon as the target materials. The CDMS experiment measures both ionization and phonon energy for each event. The majority of background particles recoil from electrons, giving a high ratio of the ionization energy to phonon recoil energy, while WIMP scattering events have low ratios because they recoil from nuclei. This signature ratio is used in background discrimination. With the measured event rates after various background cuts, the CDMS experiment is then able to draw an upper limit curve in the cross-section and WIMP mass parameter space. The CDMS result is currently the world leading limit over a wide range in the cross-section and WIMP mass parameter space.

In the SHM, the solar system is orbiting the Milky Way and therefore moving through the dark matter distribution. Earth's orbital motion around the Sun induces different relative velocities of the dark matter to Earth throughout a year, which is regarded as a signature of the existence of dark matter in the DM direct searches. The annual modulation of the dark matter flux, and thus of the observed event rates, should exhibit the expected phase and frequency. The DAMA/LIBRA experiment, an experiment in Gran Sasso, Italy searching for this annual modulation signal, employs thallium-doped sodium iodide to hunt for the WIMP-nucleon recoil event. The electrons and nuclei recoiling due to the WIMP interactions cause the emission of photons that will be detected by photomultiplier tubes. The DAMA/LIBRA experiment does not discriminate between the electron and nuclear recoils. The DAMA/LIBRA claims to observe the expected annual modulation of the dark matter [12]. This modulation reaches a maximum in June and the period is roughly a year. Nonetheless, the DAMA/LIBRA's observations are controversial as they are inconsistent with the null observations from other leading experiments, such as CDMS and XENON100. In addition, unaccounted-for background seasonal fluctuations

can also result in this annual modulation. To cross check the DAMA/LIBRA's results, physicists have been proposing a similar experiment to be located at the South Pole. The South Pole is a suitable location because background, including the muon rates and temperature, at the South Pole is opposite to that in the Northern Hemisphere. This paper is hence motivated to study the feasibility of such an experiment under various conditions.

In this paper, we first review and study the details of the standard halo model to explain the properties of the limit curves and allowed region in the cross-section and mass parameter space. We subsequently reproduce existing results from the DAMA/LIBRA experiment as a test of the programs and algorithm. At the end, we study the upper limit curve set by the modulation amplitude by varying background levels and energy thresholds.

### ***Review of Dark Matter Standard Halo Model***

As a review of the dark matter standard halo model [1], we derive the formulae necessary to understand the DM annual modulation and various background effects. In this paper, we focus on the elastic spin-independent scattering.

We begin derivation with the event rate per unit mass on a target of atomic mass  $A$  (AMU) with WIMP-nucleon cross-section  $\sigma$ , which is the characteristic area of a nucleon that quantifies the probability of an interaction.

$$dR = \frac{N_0}{A} \sigma v dn \tag{1}$$

where  $N_0 = 6.02 \times 10^{26} \text{ nuclei/kg}^{-1}$  and  $dn$  is the dark matter number density and  $v$  is the dark matter incident velocity. Note that differential event rate is linearly proportional to the cross-section. Linear rescaling can be applied manually to any figures drawn in this paper that use arbitrary cross-section in the unit of picobarn ( $\text{pb} = 10^{-36} \text{ cm}^2$ ). If the number density is

written in terms of velocity distribution, for which we adopt Maxwell–Boltzmann distribution, then

$$dn = \frac{n_0}{k} f(v, v_E) d^3v \quad (2)$$

$$f(v, v_E) = e^{-\frac{(v+v_E)^2}{v_0^2}}, \quad (3)$$

$v_E$  is the Earth (target) velocity relative to the dark matter,  $v_0$  is the width of the velocity distribution, and  $k$  is the normalization constant to satisfy the condition where

$$n_0 \equiv \int_0^{v_{esc}} dn \quad (4)$$

Thus, we solve for  $k$  in an approximation where the distribution is truncated at  $|\mathbf{v} + \mathbf{v}_E| = v_{esc}$ :

$$k = \int_0^{2\pi} d\varphi \int_0^\pi d\theta \int_0^{v_{esc}} f(v, v_E) v^2 dv \quad (5)$$

$$k = k_1 = k_0 \left[ \operatorname{erf}\left(\frac{v_{esc}}{v_0}\right) - \frac{2}{\pi^{1/2}} \frac{v_{esc}}{v_0} e^{-v_{esc}^2/v_0^2} \right] \quad (6)$$

$$k_0 = (\pi v_0^2)^{3/2} \text{ for } v_{esc} \rightarrow \infty \quad (7)$$

The cross–section is assumed to be a constant  $\sigma_0$  and  $dR$  becomes

$$dR = R_0 \frac{k_0}{k} \frac{1}{2\pi v_0^4} v f(v, v_E) d^3v \quad (8)$$

$$R_0 \equiv \frac{2}{\pi^{1/2}} \frac{N_0}{A} \sigma_0 v_0 n_0 \quad (9)$$

We want to study the event rates at different experimental energy thresholds, which set a range of the recoil energy that an experiment is sensitive to. As a result, we solve for the differential event rate  $\frac{dR}{dE_R}$  at recoil energy  $E_R$ . From kinematics we know that  $E_R = rE(1 - \cos \theta)/2$  and  $r = \frac{4M_D M_T}{(M_D + M_T)^2}$  where  $E = \frac{1}{2} M_D v^2$  is the dark matter incident energy and  $M_T$  is the target mass.

$$\frac{dR}{dE_R} = \int_{E_{min}}^{E_{max}} \frac{1}{rE} dR(E) = \frac{1}{rE_0} \int_{v_{min}}^{v_{max}} \frac{v_0^2}{v^2} dR(v) \quad (10)$$

where  $E_{min} = E_R/r$ , the minimum dark matter energy that can deposit a recoil energy of  $E_R$ , i.e.

$$v_{min} = v_0 \left( \frac{E_R}{rE_0} \right)^{1/2}, \text{ where } v_0 = 220 \text{ km/s as used in [13].} \quad (11)$$

$$\frac{dR}{dE_R} = \frac{R_0}{rE_0} \frac{k_0}{k} \frac{1}{2\pi v_0^2} \int_{v_{min}}^{v_{max}} \frac{1}{v} f(v, v_E) d^3v \quad (12)$$

$$\frac{dR(v_E, \infty)}{dE_R} = \frac{R_0}{rE_0} \frac{\pi^{1/2}}{4} \frac{v_0}{v_E} \left[ \text{erf} \left( \frac{v_{min} + v_E}{v_0} \right) - \text{erf} \left( \frac{v_{min} - v_E}{v_0} \right) \right] \quad (13)$$

$$\frac{dR(v_E, v_{esc})}{dE_R} = \frac{k_0}{k_1} \left[ \frac{dR(v_E, \infty)}{dE_R} - \frac{R_0}{rE_0} e^{-v_{esc}^2/v_0^2} \right] \quad (14)$$

We have obtained the equation of the differential event rate as a function of  $v_E$  and  $v_{esc}$ , and  $v_{esc} = 650 \text{ km/s}$  as used in [13]. To compare the experimental event rates, one needs to integrate this function with respect to recoil energy over the energy thresholds because each experiment has its sensitive energy interval. The Earth velocity in galactic coordinates as a function of time is given in Ref. [1] and plotted in Fig. 1.

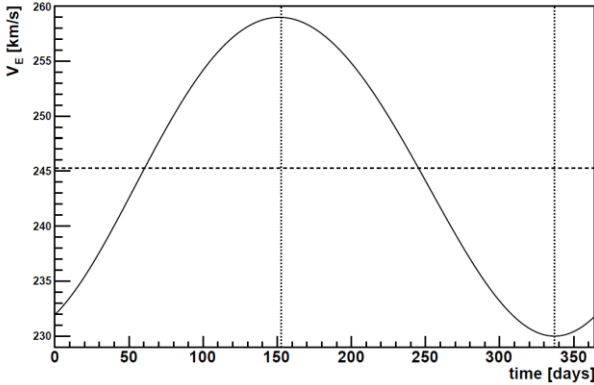


Fig. 1. Earth velocity relative to the dark matter halo, which reaches maximum in June and minimum in December.

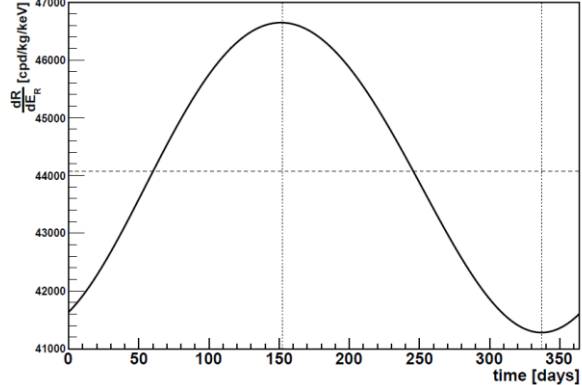


Fig. 2. The even rate as a function of time drawn at  $\sigma = \text{unit pb}$  and  $m_X = 50 \text{ GeV}$ . This oscillates according to the Earth velocity.

The Earth velocity relative to the dark matter halo in Fig. 1 peaks on the 153th day, corresponding to June 2<sup>nd</sup>, and reaches the minimum on the 336<sup>th</sup> day, corresponding to December 2<sup>nd</sup>. The average velocity occurs on March 1<sup>st</sup>. The incident velocities of the dark

matter, and thus the event rates, differ with Earth velocity. The difference in the differential event rate at different velocities is illustrated in Fig. 3 for iodine.

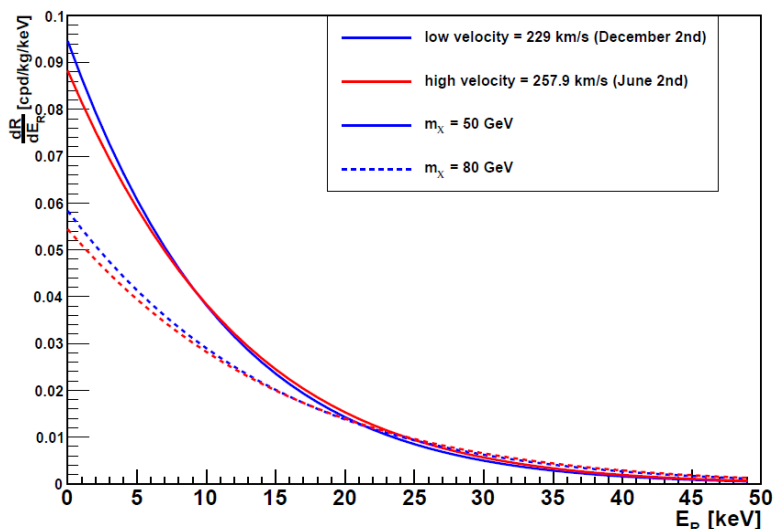


Fig. 3. Differential event rate of iodine with  $\sigma = 1 \times 10^{-6} pb$  as a function of its recoil energy.

To understand the details of the later figures, we now study the properties of the material NaI ( $A_I = 126.9$ ,  $A_{Na} = 23.0$ ) that the DAMA/LIBRA employs. The modulation seen by sodium can— for example, in WIMP mass range around 60–140 GeV for the 2–4 keV electron

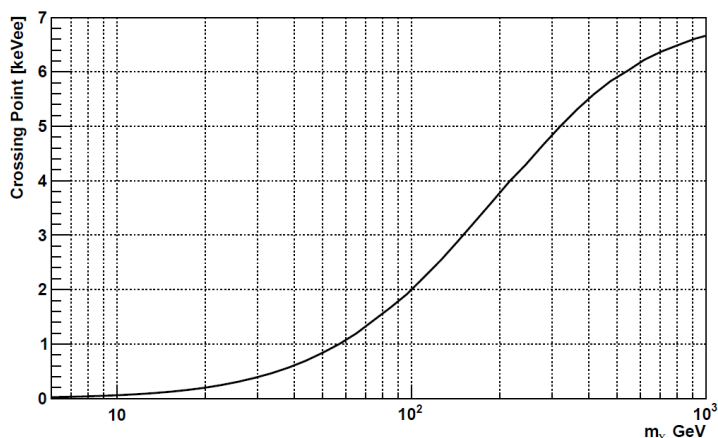


Fig. 4. This shows at what energy the intersecting point in Fig. 3 occurs for a given dark matter mass. This crossing point is important because it affects or even flips the modulation amplitude.

equivalent (keVee) energy threshold— be opposite to the one by iodine. The energy unit, keV electron equivalent, is the experimentally measured electron recoil energy calibrated using radioactive sources, and can be converted to recoil energy (keVr) of a specific target material.

This opposite modulation happens because, for the same energy range in keVee, Na’s recoil energy thresholds are lower and the modulation is opposite on the left of the crossing point in Fig.

3. For the 2–4 keVee energy range, iodine does not shift modulation until roughly 140 GeV. However, the net modulation still peaks according to iodine’s detection since iodine’s event rate is dominantly higher for its high cross–section. We refer to Fig. 4 for crossing points of NaI as a function of WIMP mass. The cause of this phenomenon is: High WIMP velocities typically cause high event rates. However, it becomes opposite when the recoil energy is low because high energy WIMPs have lower probability of causing such low recoil energy.

Although iodine has significantly higher event rates, iodine’s total event rate vanishes at the WIMP mass of around 20 GeV, higher than Na’s critical WIMP mass of around 6 GeV. This occurs because at low WIMP masses, the minimum velocity of the WIMPs that can cause the minimum recoil energy (the lower limit of the energy threshold), has exceeded  $v_{esc}$ . As a result, only Na detection remains and this is the reason why two patches/curve sections appear in the DAMA/LIBRA’s allowed region/upper limit curve plots.

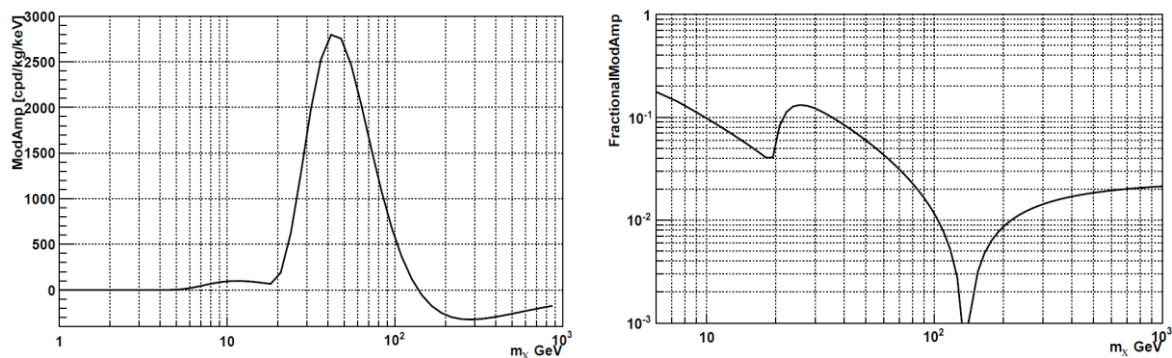


Fig. 5 (left) and 6 (right) show NaI’s theoretical absolute and relative modulation amplitude with the unit pb cross–section and 2–4 keVee energy threshold. We can again see the modulation phase shifting at the mass of around 140 GeV. In addition, we can see the critical points at around 20 and 5 GeV where iodine’s and sodium’s event rates vanish respectively.

## METHODS

### A. Reproduction of Existing Results

#### DAMA/LIBRA Allowed Region— Modulation Amplitude Spectrum Fitting

We apply the fitting algorithm to the modulation amplitude versus energy bins spectrum, as provided by DAMA/LIBRA[16]. Since DAMA energy threshold has been taken in terms of keVee, we apply quenching factors  $Q = \frac{E_{det}}{E_R}$  [keVee/keVr], (0.3 keVee/keVr for sodium and 0.09 keVee/keVr for iodine [14]) to convert the energy threshold to recoil energies. To allow direct comparison with Ref. [13], we follow the efficiency of 1 and the energy resolution is given by a Gaussian distribution with standard deviation of

$$\sigma(E) = (0.448 \text{ keVee})\sqrt{E/\text{keVee}} + 0.0091E \quad \text{in Ref. [13]}. \quad (15)$$

In the Fig. 7, negativity of the modulation amplitudes represents the opposite modulation signal. This opposite signal happens because the recoil energy is lower than the crossing point. The best-fit mass and cross-section is slightly discrepant by 2% and 6% from the ones in Ref. [13], whose result is however within the uncertainty range of this fitting result. Based on the fitting algorithm, both fitted cross-section and WIMP mass have uncertainties at the order of 10% so this may give later results a systematic uncertainty of 10% in both best-fit quantities.

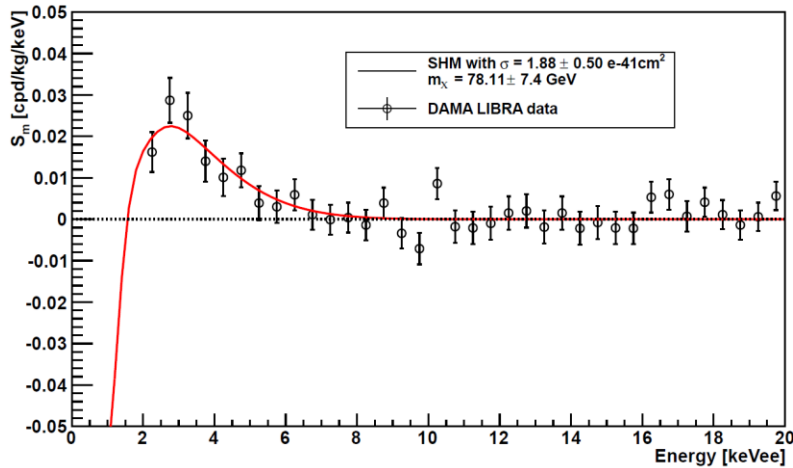


Fig. 7. A  $\chi^2$  fit to the data reported by the DAMA/LIBRA.

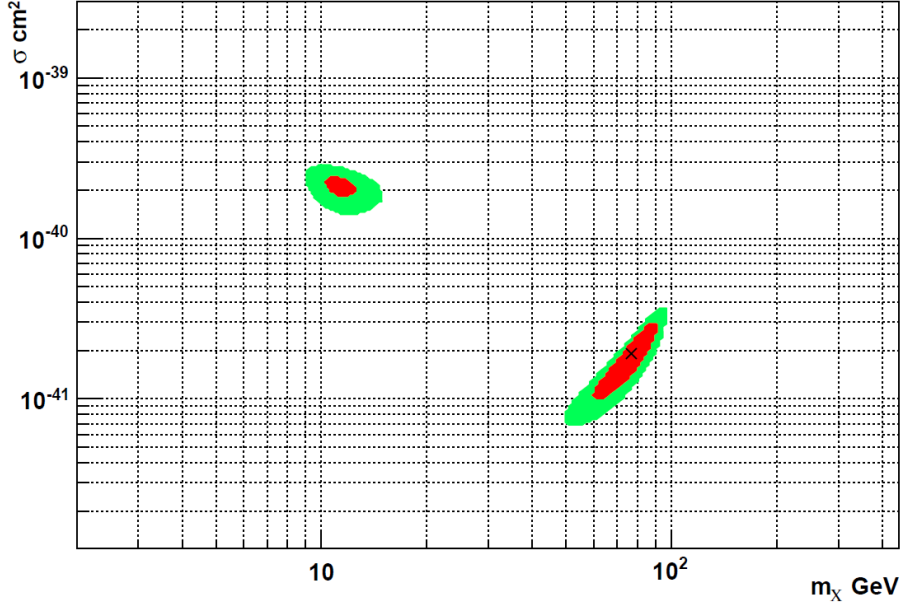


Fig. 8. The allowed region is drawn using the  $\chi^2 \leq \chi_{\min}^2 + \Delta\chi^2$  method at 90% C.L. and  $3\sigma$  level.  $\Delta\chi^2 = 4.61$  and  $11.83$  respectively for this two-parameter ( $\sigma$  &  $m_\chi$ ) fitting.

### ***B. Sensitivity Curves—the Setup of the Algorithm***

With data randomly generated from a Poisson distribution that assumes zero signal and various background levels, we apply a fitting algorithm similar to the one discussed for DAMA/LIBRA. In this fitting scenario, however, we adopt cosine as an approximation of the modulation fitting function. The upper limit of modulation amplitude at 90% C.L. is taken to be  $1.64 \times \sigma_{\text{error}}$ , where  $\sigma_{\text{error}}$  is the error associated with the amplitude of the fit. For large number of trials, the spectrum of the fit values will approach to a Gaussian distribution with the width  $\sigma_{\text{error}}$ . Thus, the amplitude  $1.64 \times \sigma_{\text{error}}$  corresponds to 90% C.L. With this limit metric, we generate upper limits curve for a generic NaI experiment as shown in Fig 9.

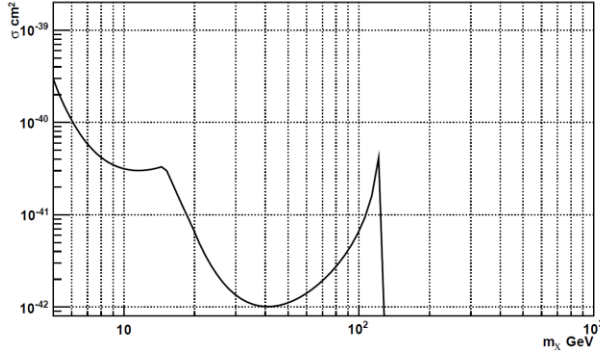


Fig. 9. Upper limit set by modulation amplitude at 0.5 counts per day/kg/keVee (cpd/kg/keV, for short).

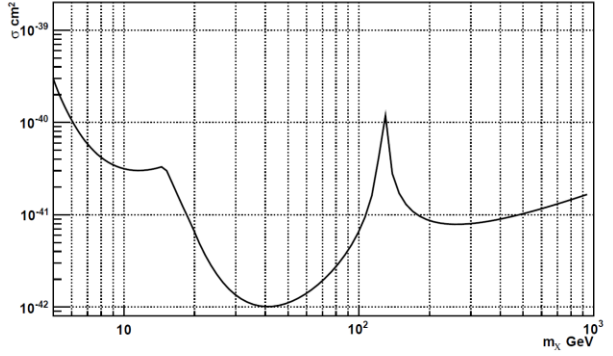


Fig. 10. Same upper limit but the amplitude is taken absolute value. The total rate limit has not been set.

The sudden decline at around 200 GeV shows where the modulation signal shifts  $180^\circ$  in phase at high mass regions. To obtain Fig. 10, we take the absolute value of the modulation amplitude fitted on random background events. Furthermore, the kink at the shifting point is better constrained by the total event rate to obtain the final sensitivity curves in the result section.

## RESULTS

### *Sensitivity Curve for Zero Signal and Various Background Levels*

First, we study how running an experiment longer or with a larger target mass can help improve its sensitivity. The exposure is defined as the product of the mass of the target materials and the exposure time. As discussed in the method section B, with this zero signal assumption, the upper limit is proportional to the error of the fit, which is then proportional to the reciprocal of the square root of the number of events/exposure (Fig. 11 as an example). For a background

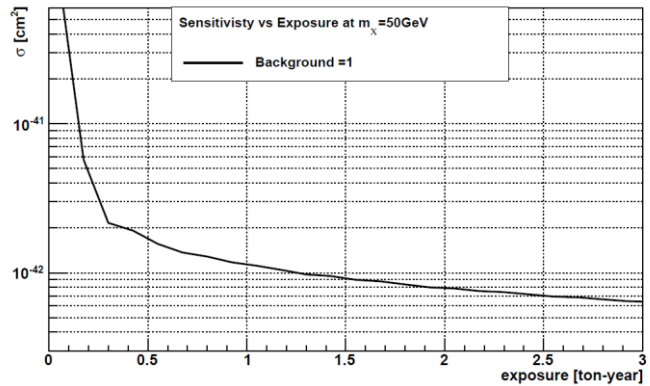


Fig. 11. This limit versus exposure curve with WIMP mass of 50 GeV shows that experiments cannot improve the sensitivity much by extending exposure time.

limited experiment, the sensitivity eventually reaches to a limit caused by its background rate. For a 250 kg NaI experiment with a background, the sensitivity to annual modulation is not improved significantly by increasing the exposure time beyond 1 year. Therefore, with little help from extending exposure time, we turn to explore the effects of other experimental controls—background levels and energy thresholds— with a fixed two-year exposure time and the target mass of 250 kg.

### *1. Background Levels*

For direct comparison with the CDMS experiment limit, we include the limit curve obtained from the cumulative exposure of CDMS II [17] in the following figures. The energy interval for NaI is set to be 2–4 keV because the WIMP signal is strong at low recoil energy and a lower energy threshold is experimentally difficult to achieve. The background levels of this investigation range from 0.5 cpd/kg/keV— the DAMA/LIBRA’s range [15]— to 10 cpd/kg/keV— roughly the NAIAD experiment’s background level [18]. We expect the background levels of proposed experiments to fall into this range.

From Fig. 12, we see that iodine’s allowed region is deep in the CDMS’s excluded region. As a result, we focus on the allowed region of Na (low WIMP mass) because there is controversy [13] over whether this allowed region has been ruled out.

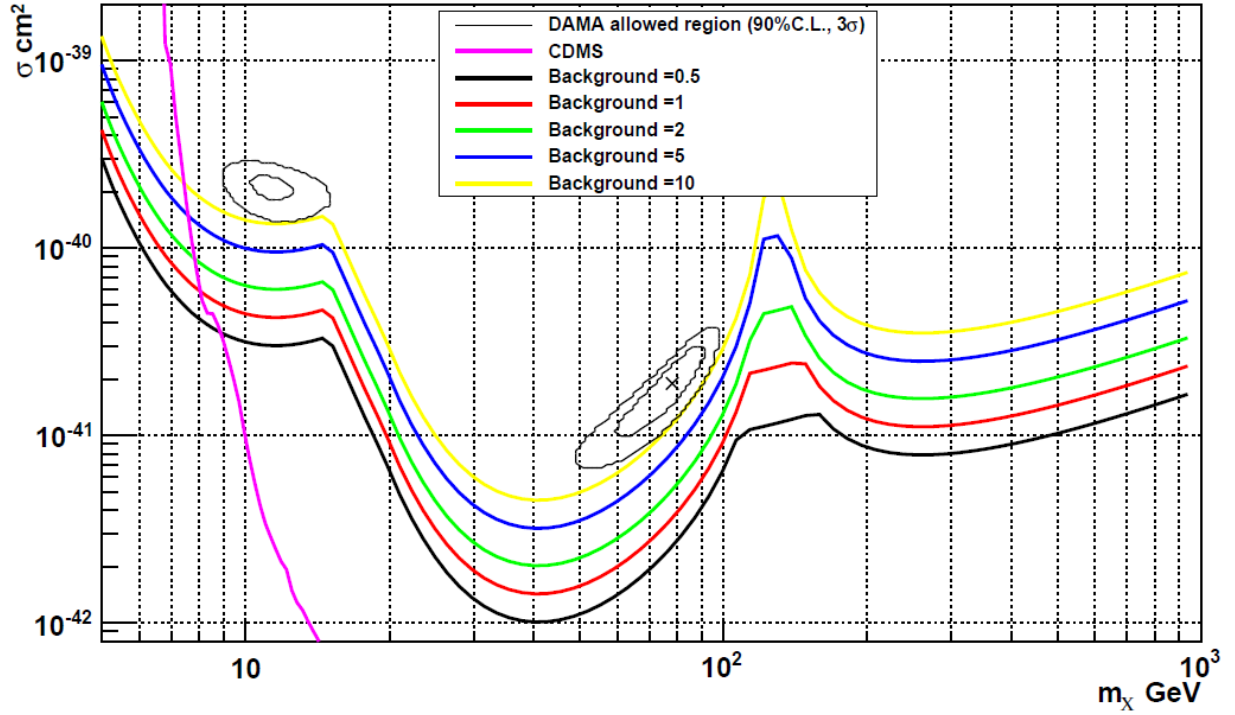


Fig. 12. Energy threshold: 2–4 keVee. This figure shows how sensitivity is improved by suppressing the background to different levels.

We explore five different background levels for a hypothetical NaI detector. In Fig. 12, we apply the techniques discussed in the method section B to obtain the upper limit curve. We generate Fig. 13 to study the dependence of cross-section on background at a fixed WIMP mass—50 GeV.

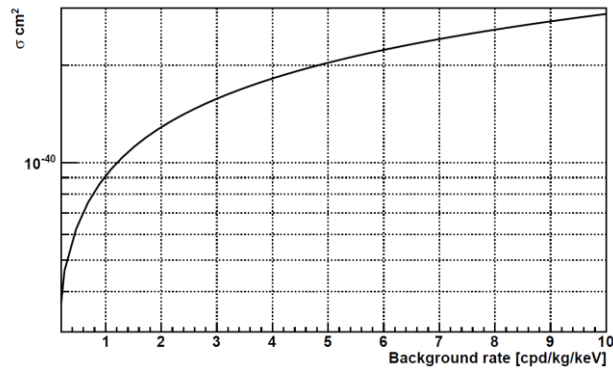


Fig. 13. At  $m_\chi = 50 \text{ GeV}$ . This natural logarithm result is as expected because the error in modulation amplitude, therefore upper limit, is proportional to  $\sqrt{N_{events}}$  and  $N_{events}$  is linearly dependent on background rate under zero DM signal assumption.

## 2. Energy Thresholds

Now we explore the effects of varying the energy thresholds– 1–6, 2–6, 3–6, and 4–6 keVee in this section. These ranges are of our interests because the DAMA and NAIAD experiments can lower their energy thresholds down to 2 keVee and 4 keVee respectively whereas 1 keVee will be an ideal case. To obtain the sensitivity curves calculated from the upper limits of the modulation amplitude for the hypothetical NaI detector, the energy resolution in Eqn. 15 has been applied.

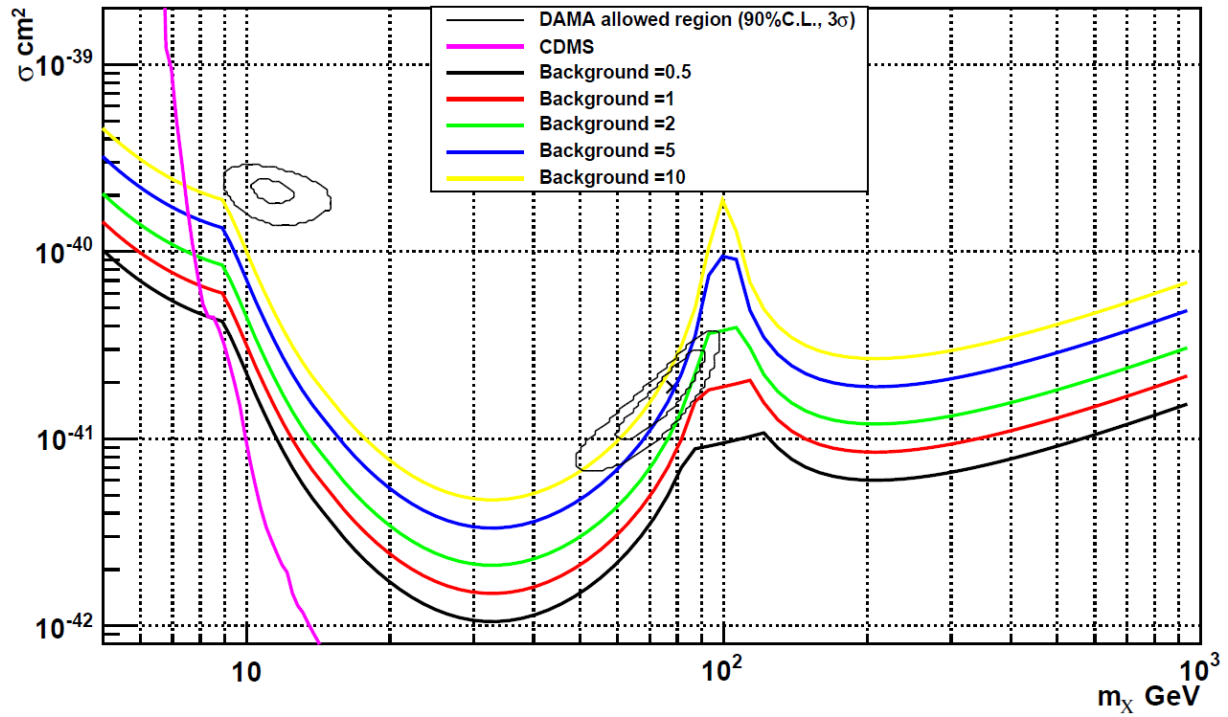


Fig. 14. Energy threshold: 1–6 keVee.

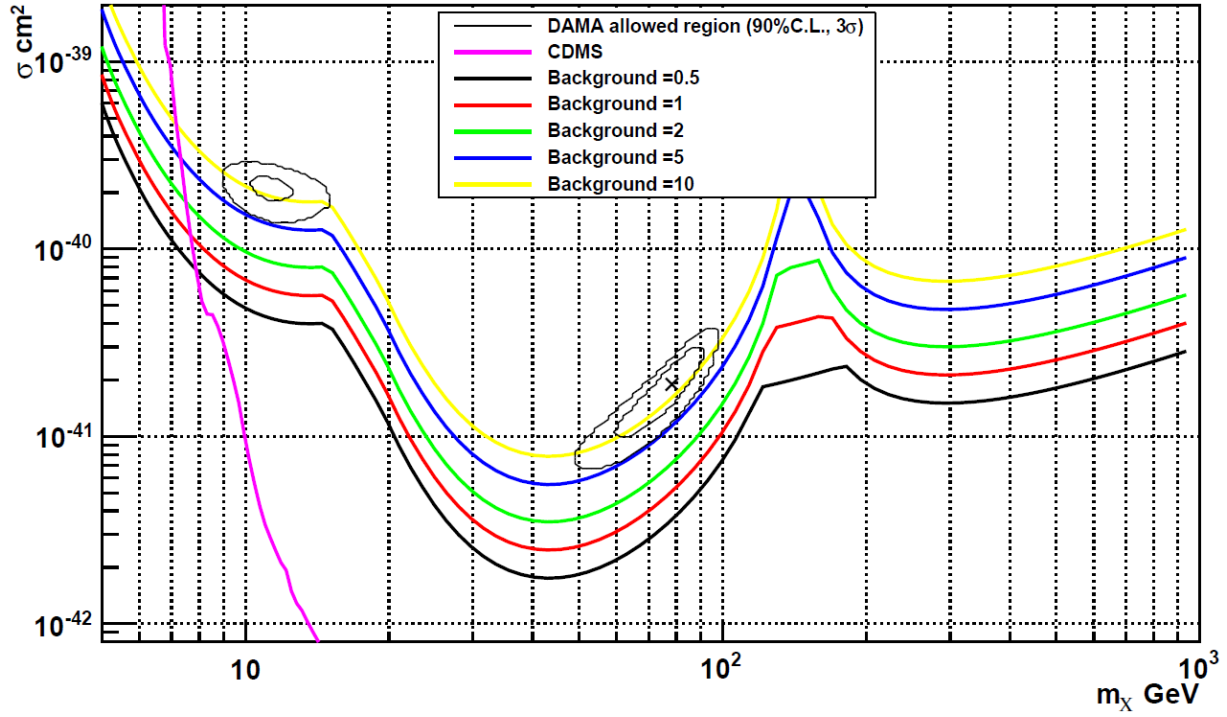


Fig. 15. Energy threshold: 2–6 keVee.

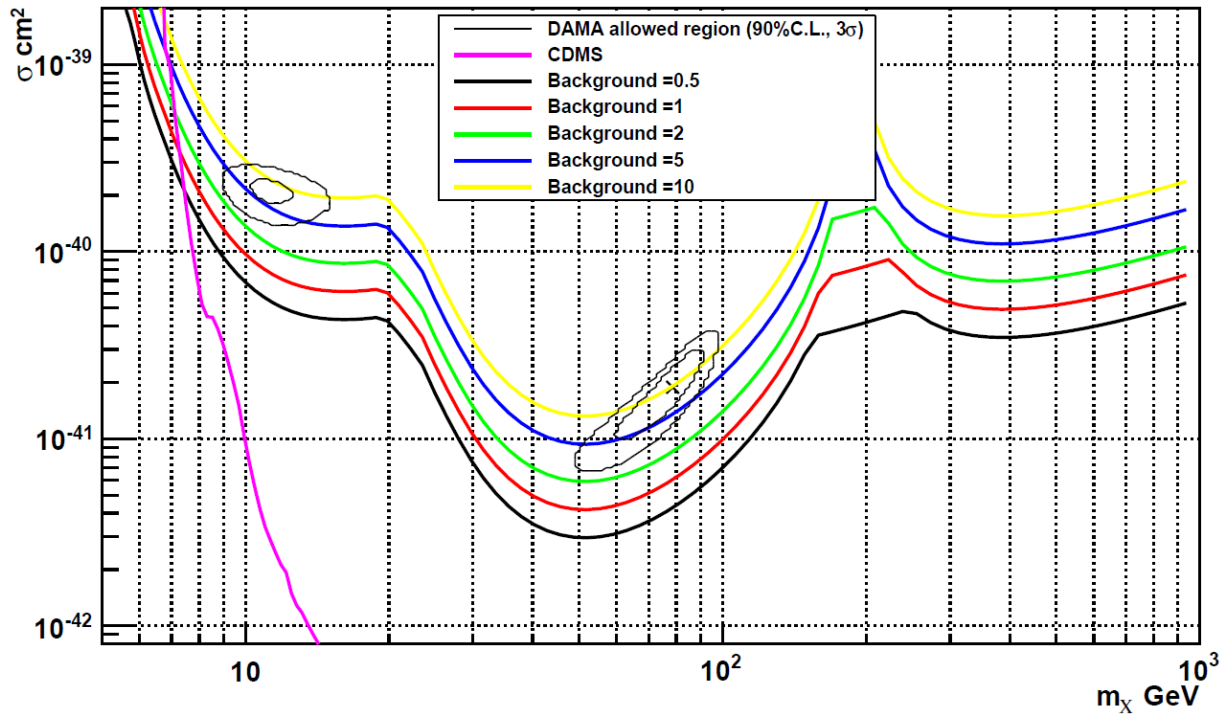


Fig. 16. Energy threshold: 3–6 keVee.

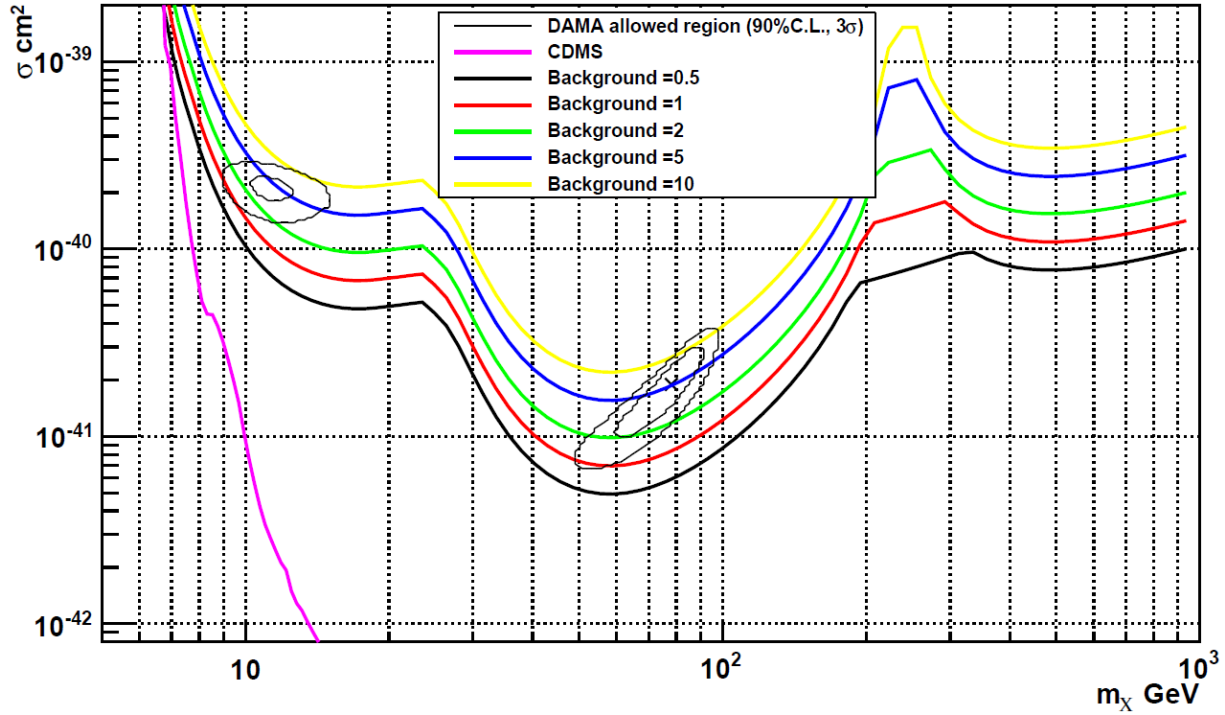


Fig. 17. Energy threshold: 4–6 keVee.

The energy threshold 1–6 keVee generates the most sensitive curve (Fig. 14) in a wide range of the parameter space albeit not in the entire WIMP mass spectrum. It loses the sensitivity at its crossing point region (refer to discussion on Fig. 3). At low WIMP mass regions, the sensitivity highly depends on the low energy thresholds. We also notice that each energy interval’s region where low sensitivity occurs due to crossing point in Fig. 3 shifts to higher WIMP masses from low energy interval to higher (Fig. 14 to 17) as expected from Fig. 4.

## DISCUSSION & CONCLUSION

The motivation of this paper is to investigate necessary conditions that allow future proposed experiments to probe the DAMA/LIBRA allowed region. An experiment has, at some degree, control over such parameters as the exposure, reduction of background level, energy thresholds, and energy binning. Hence, it is important to gauge the influence of each of these

variables to find the best strategy for each experiment that is cross-checking the DAMA/LIBRA's annual modulation observation.

To exclude the DAMA/LIBRA's Na allowed region, (Fig. 14–17), with null observation of the annual modulation, the maximum allowed background level, at each confidence level, has to be suppressed to the corresponding value in Table 1 (in terms of cpd/kg/keV). The DAMA/LIBRA experiment has low energy threshold 2 keVee with background less than 1 cpd/kg/keV [15] while the NAIAD experiment has energy threshold of 4 keVee with roughly 10 cpd/kg/keV background level [18]. Therefore, these conditions are experimentally achievable.

|                              | 1–6 keVee | 2–6 keVee | 3–6 keVee | 4–6 keVee |
|------------------------------|-----------|-----------|-----------|-----------|
| At 90% C.L.                  | >10       | 10        | 5         | 2         |
| At 99.73% C.L. ( $3\sigma$ ) | 10        | 5         | 2         | 1         |

Table 1 Maximum allowed background levels (cpd/kg/keV) at a given confidence level and an energy threshold.

By comparing different energy thresholds, we realize that the low limit of the energy threshold is also a key to increasing the experiment's sensitivity in probing not only the DAMA/LIBRA's allowed region but also new parameter space. Lower energy thresholds enhance the sensitivity because of the high expected event rates at low recoil energies (Fig. 3). Nevertheless, a low energy threshold (1–6 keVee, for example) does not necessarily serve as a better condition over the entire parameter space for the following reason: an energy range that includes crossing point (refer to Fig. 3 and 4) will result in the cancellation of the modulation amplitude and therefore a lower sensitivity.

Nonetheless, the energy bins too far above the crossing point will instead cause the loss of event rate (Fig. 3) and hence a low sensitivity as well. More specifically, we know (Fig. 4) that the crossing point for the 1–6 keVee interval occurs within these energy thresholds over the WIMP mass range of 50 to 540 GeV. This demonstrates its high sensitivity at low masses (<50GeV) but suffers from a poor sensitivity around its crossing region ( $\approx 100\text{GeV}$ ).

Consequently, a wise strategy for the experiments that search for annual modulation in general, is that energy binning should be applied to optimize the sensitivity provided by the data. For the maximum possible modulation signal, the division point of the energy binning should be taken according to the Fig. 4 (for NaI) to separate two opposite modulation contributions.

Conclusively, we have studied the dark matter standard halo model and the properties of NaI, and discovered some interesting experimental techniques that can improve the limitation of the experiments. Many strategies, including the experiments exposure time, background suppression, energy threshold limit, and energy binning techniques, have been discussed and they should be taken into account in the purposed experiments that are to unveil the mystery of dark matter by hunting for the annual modulation signature.

## **ACKNOWLEDGEMENT**

This research is conducted at Fermi National Accelerator Laboratory. I am wholeheartedly grateful to my mentors, Drs. Jonghee Yoo and Lauren Hsu for the proposal of this project and the enthusiastic guidance on the knowledge necessary for this feasibility analysis. I would also like to gratefully acknowledge the U.S. Department of Energy, the sponsor of the Science Undergraduate Laboratory Internship (SULI) program for funding the program. Many thanks go to the SULI coordinators, Drs. Erik Ramberg, Roger Dixon, and Eric Prebys, for providing me with such valuable educational and research experiences.

## REFERENCES

- [1] J. D. Lewin and P. F. Smith *Astropart. Phys.*, 6, 87 (1996)
- [2] V. Rubin, A. Waterman, J. Kenney, astro-ph/9904050.
- [3] F. Zwicky, *ApJ* 86, 217 (1937).
- [4] [http://heasarc.gsfc.nasa.gov/docs/rosat/gallery/clus\\_coma.html](http://heasarc.gsfc.nasa.gov/docs/rosat/gallery/clus_coma.html)
- [5] <http://www.bell-labs.com/org/physicalsciences/projects/darkmatter/darkmatter1.html>
- [6] Spergel et al., *Astrophys. J. Suppl.* 148 (2003) 175 [astro-ph/0302209]
- [7] S. Perlmutter et al., *Astrophys. J.* 517 (1999) 565 [astro-ph/9812133]
- [8] M. Tegmark et al., *Phys. Rev. D* 69 (2004) 103501 [astro-ph/0310723]
- [9] D.J. Eisenstein et al., *Astrophys. J.* 633 (2005) 560 [astro-ph/0501171]
- [10] L. Fu et al., *Astron. Astrophys.* 479 (2008) 9 [arXiv:0712.0884]
- [11] H. Goldberg, *Phys. Rev. Lett.* 50, 1419 (1983) and J. Ellis, J. Hagelin, D. V. Nanopoulos and M. Srednicki, *Phys. Lett.* B127, 233 (1983).
- [12] R. Bernabei et al., arXiv:1002.1028v1
- [13] C. Savage et al., arXiv:0808.3607v3
- [14] R. Bernabei et al., *Phys. Lett.* B389:757–766 1996
- [15] R. Bernabei et al., arXiv:astro-ph/0311046v1
- [16] R. Bernabei et al., *Eur. Phys. J. C* 67 (2010) 39.
- [17] Z. Aham et al., *Science* 327 (5973), 1619.
- [18] G.J. Alner et al., *Phys. Lett.* B616 (2005) 17–24